SRF 970314-01

Coherent Synchrotron Frequency Shift due to the Fundamental Accelerating Cavity Mode in CESR.

S. Belomestnykh
Laboratory of Nuclear Studies, Cornell University, Ithaca, NY 14853

1 Introduction

A coupled-bunch longitudinal instability observed in CESR with 9 trains of 2 bunches is presently a limitation for a total beam current [1]. Machine studies are in progress to understand the cause of the instability and to find a cure. At the same time our attention was brought to the big frequency shift of the lowest longitudinal coupled bunch mode of oscillations. It turned out that the last phenomenon is well known and well understood as an interaction of the beam with accelerating cavity fundamental mode. Due to the active RF system, beam interaction with the fundamental mode of accelerating cavity differs from interaction with higher-order modes (HOMs). I wrote this note at the request of several people to have some readily available analysis on the matter. First, I briefly explain some theory, then report results of measurements in CESR and compare those results with simple analytic estimation and results obtained with computer codes. Finally, predictions for the superconducting RF (SRF) cavities are presented.

I use following definition of the cavity specific impedance, R/Q:

$$R/Q = \frac{V_c^2}{2\omega_r U},$$

where U is the stored energy, ω_r is the resonant angular frequency, and V_c is the amplitude of the cavity voltage. Also, I chose the origin of the coordinate system at the null of the RF wave as it is shown in Figure 1. Table 1 lists some parameters of the CESR beam and RF systems relevant to calculations in this paper.

2 Coupled-bunch Longitudinal Oscillations

Instabilities cased by the electromagnetic interaction of bunched beam with various discontinuities of the vacuum chamber is one of the main factors limiting the beam intensity in a storage ring. Such an interaction with RF cavity or any other narrow-band insertion can cause longitudinal or transverse instability of a beam motion. The beam remains stable if synchrotron radiation (SR) or Landau damping time is smaller than the instability growth time.

As far as we are interested in longitudinal case in this paper, let us consider the theory for this case. The theory for a single-bunch or multi-bunch beam (with equally spaced bunches) has been developed by several authors (see, for example, [2], [3], [4]). We will focus on a macroparticle model for simplicity. In this model rigid, structureless bunches of the beam interact with their own wake field. One can find good description of this model in [5].

2.1 Robinson Instability

Let us consider a single-bunch beam interacting with a narrow-band resonance. The revolution time of a particle bunch depends on the average energy of particles within a bunch and the Fourier spectrum of the bunch current being made up of harmonics of the revolution frequency is therefore energy dependent. On the other hand, by virtue of the frequency dependence of the cavity impedance, the energy loss of a bunch in the cavity depends on the revolution frequency. We have therefore an energy dependent loss mechanism which can led to damping or untidamping of *coherent phase oscillations* (longitudinal oscillations). This effect is generally referred to as *Robinson instability.*

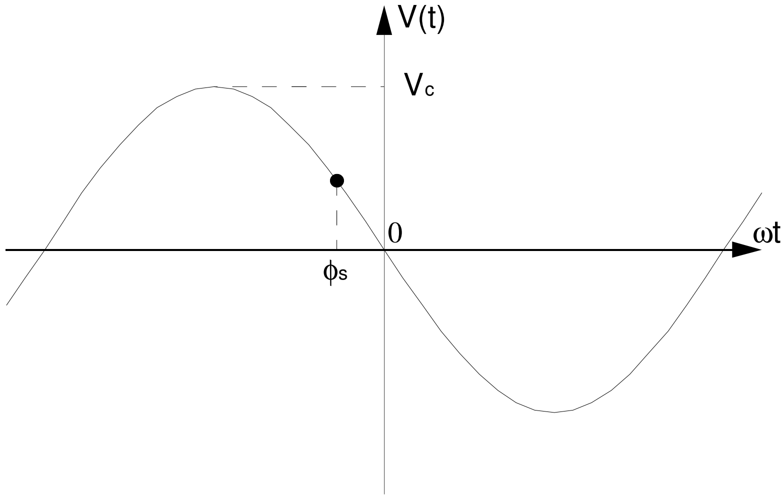

Figure 1: Coordinate system for the RF wave.

Table 1: Selected parameters of the CESR beam and RF systems.

Beam energy, E	5.3 GeV
SR energy loss per turn, U_0	1.2 MeV/turn
Momentum compaction, α	0.0113
RF frequency, f_{RF}	499.765 MHz
RF harmonic number, h	1281
NRF:	
Total operating voltage, V_c	6.0 MV
R/Q (per cell)	128 Ohm
Unloaded quality factor, Q_0	3.17×10^4
Coupling coefficient, β_0	5.0
No. of cavities	4
No. of cells per cavity	5
SRF:	
Total operating voltage, V_c	7.2 MV
R/Q (per cell)	44.5 Ohm
Unloaded quality factor, Q_0	10^9
Coupling coefficient, β_0	5×10^3
No. of cavities	4
No. of cells per cavity	1

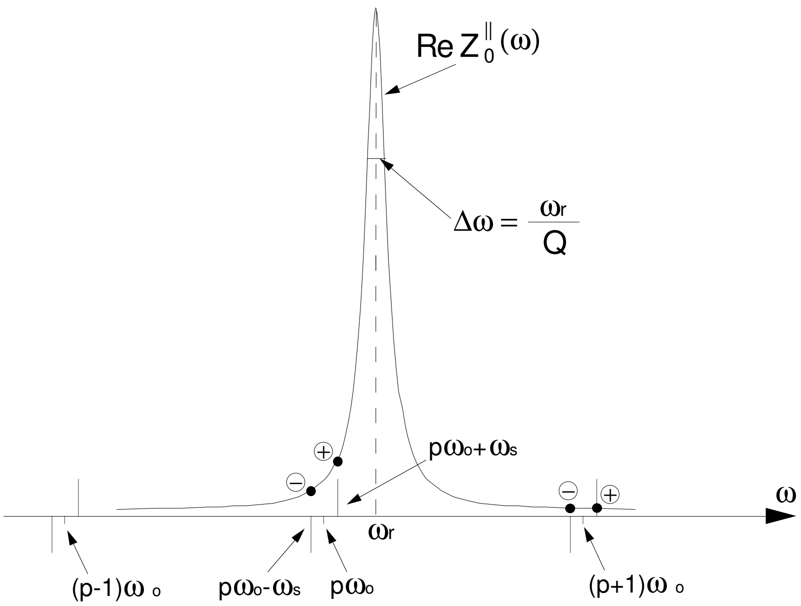

Figure 2: Robinson instability: narrow-band resonance, $\omega_r > p\omega_0$.

The exact location of resonant frequency ω_r relative to the nearest harmonic of revolution frequency $p\omega_0$ is of critical importance for the stability of the beam. Above the transition energy, the beam will be unstable if ω_r is slightly above $p\omega_0$ and stable if slightly below. Figure 2 shows the case of unstable situation. One can calculate an *instability growth rate* using formula

$$\tau^{-1} = \omega_s \frac{I_0}{2hV_c\cos(\phi_s)\omega_0} \sum_{p=-\infty}^{\infty} (p\omega_0+\omega_s) ReZ_0^{||}(p\omega_0+\omega_s) \tag{1}$$

$$= \omega_s \frac{I_0}{2hV_c\cos(\phi_s)\omega_0} \sum_{p=0}^{\infty} \Big[(p\omega_0+\omega_s) ReZ_0^{||}(p\omega_0+\omega_s) - (p\omega_0-\omega_s) ReZ_0^{||}(p\omega_0-\omega_s)\Big] \tag{2}$$

$$\approx \omega_s \frac{I_0}{2hV_c\cos(\phi_s)} \sum_{p=0}^{\infty} p\left[ReZ_0^{||}(p\omega_0+\omega_s) - ReZ_0^{||}(p\omega_0-\omega_s)\right], \tag{3}$$

where ω_s is the the synchrotron oscillation frequency, I_0 is the total beam current, h is the RF harmonic number, ϕ_s is the synchronous phase, and $Z_0^{||}(\omega)$ is the cavity impedance.

On the other hand, this interaction perturbes the frequency of synchrotron oscillations and we can get a *frequency shift*

$$\Delta\Omega = \omega_s \frac{I_0}{2hV_c\cos(\phi_s)\omega_0} \sum_{p=-\infty}^{\infty} \Big[p\omega_0 ImZ_0^{||}(p\omega_0) - (p\omega_0+\omega_s) ImZ_0^{||}(p\omega_0+\omega_s)\Big] \tag{4}$$

$$= \omega_s \frac{I_0}{2hV_c\cos(\phi_s)\omega_0} \sum_{p=0}^{\infty} \Big[2p\omega_0 ImZ_0^{||}(p\omega_0) - (p\omega_0+\omega_s) ImZ_0^{||}(p\omega_0+\omega_s) - (p\omega_0-\omega_s) ImZ_0^{||}(p\omega_0-\omega_s)\Big] \tag{5}$$

$$\approx \omega_s \frac{I_0}{2hV_c\cos(\phi_s)} \sum_{p=0}^{\infty} p\left[2ImZ_0^{||}(p\omega_0) - ImZ_0^{||}(p\omega_0+\omega_s) - ImZ_0^{||}(p\omega_0-\omega_s)\right] \tag{6}$$

There are two terms under the summation in the last formula. The first term, called *incoherent frequency shift*, comes from a potential-well distortion, while the origin of the second term, which is *coherent frequency shift*, is dynamical. The static potential-well distortion does not contribute to the growth rate.

Thus, we see that the coherent frequency shift depends on the behaviour of the imaginary part of the cavity impedance on the synchrotron side bands of the harmonics of revolution frequency. One can see from (6) that incoherent term will almost compensate coherent term if ω_r is far away from harmonics of revolution frequency.

2.2 Multi-bunch Case: Equally-spaced, Equally-populated Bunches

One can easily generalize approach from the single-bunch case to this case (see, for example, [4]). If we have M bunches then we immediately get M coupled-bunch modes with the phase shift between adjacent bunches for the mode number n

$$\Delta\phi_n = \frac{2\pi}{M}n, \quad n = 0, 1, \ldots, M-1$$

and formulae for the growth rate and frequency shift

$$\begin{aligned}
\tau_n^{-1} &= \omega_s \frac{I_0}{2hV_c\cos(\phi_s)\omega_0} \sum_{p=-\infty}^{\infty} (pM\omega_0 + n\omega_0 + \omega_s) Re Z_0^{\|}(pM\omega_0 + n\omega_0 + \omega_s) && (7) \\
&= \omega_s \frac{I_0}{2hV_c\cos(\phi_s)\omega_0} \times \\
&\quad \times \sum_{p=0}^{\infty} \Big[(pM\omega_0 + n\omega_0 + \omega_s) Re Z_0^{\|}(pM\omega_0 + n\omega_0 + \omega_s) - (pM\omega_0 - n\omega_0 - \omega_s) Re Z_0^{\|}(pM\omega_0 - n\omega_0 - \omega_s)\Big] && (8) \\
&\approx \omega_s \frac{I_0}{2hV_c\cos(\phi_s)} \sum_{p=0}^{\infty} \Big[(pM + n) Re Z_0^{\|}(pM\omega_0 + n\omega_0 + \omega_s) - (pM - n) Re Z_0^{\|}(pM\omega_0 - n\omega_0 - \omega_s)\Big] && (9)
\end{aligned}$$

$$\begin{aligned}
\Delta\Omega &= \omega_s \frac{I_0}{2hV_c\cos(\phi_s)\omega_0} \sum_{p=-\infty}^{\infty} \Big[pM\omega_0 Im Z_0^{\|}(p\omega_0) - (pM\omega_0 + n\omega_0 + \omega_s) Im Z_0^{\|}(pM\omega_0 + n\omega_0 + \omega_s)\Big] && (10) \\
&= \omega_s \frac{I_0}{2hV_c\cos(\phi_s)\omega_0} \sum_{p=0}^{\infty} \Big[2pM\omega_0 Im Z_0^{\|}(pM\omega_0) - \\
&\quad - (pM\omega_0 + n\omega_0 + \omega_s) Im Z_0^{\|}(pM\omega_0 + n\omega_0 + \omega_s) - (pM\omega_0 - n\omega_0 - \omega_s) Im Z_0^{\|}(pM\omega_0 - n\omega_0 - \omega_s)\Big] && (11) \\
&\approx \omega_s \frac{I_0}{2hV_c\cos(\phi_s)} \sum_{p=0}^{\infty} \Big[2pM Im Z_0^{\|}(pM\omega_0) - \\
&\quad - (pM + n) Im Z_0^{\|}(pM\omega_0 + n\omega_0 + \omega_s) - (pM - n) Im Z_0^{\|}(pM\omega_0 - n\omega_0 - \omega_s)\Big] && (12)
\end{aligned}$$

Figure 3 shows example for the case of four bunches. One can see that only 0 and π modes ($n = 0$ and $n = \frac{M}{2}$ have contributions from the sidebands of the same harmonic of revolution frequency. Usually about one half of the coupled bunch modes are stable and one half are unstable.

2.3 Multi-bunch Case: Non-equal and/or Non-equally Spaced Bunches

A general approach to the case of non-equal, non-equally spaced bunches in the counter-rotating beams was developed in [6]. Another formulation, for bunch trains, was developed recently by M. Billing and is described in [7]. I won't discuss this case and refer the reader to the cited references.

3 Detuning of the Fundamental Cavity Mode due to the Beam Loading

The cavity tuning in storage rings is usually set to minimize reflection from the cavity. The resonant frequency is detuned toward the lower side to compensate the reactive component of the beam loading. The shift of the resonant frequency for an optimum operation is given by

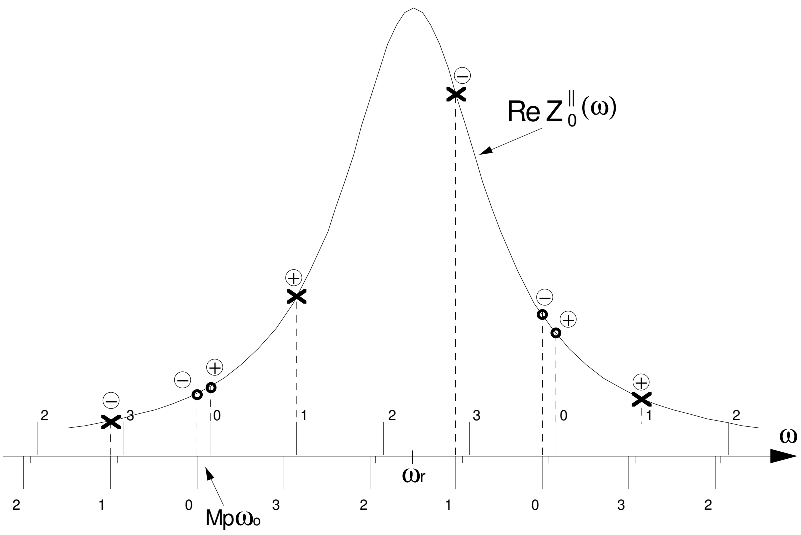

Figure 3: Coupled-bunch modes for $M = 4$ bunches: contributions for $n = 0$ mode (circles) and $n = 1$ mode (crosses), wide-band resonance.

$$\Delta f_r = -f_{RF} \frac{I_0 \cos(\phi_s)}{V_c} \frac{R}{Q}, \tag{13}$$

$$\sin(\phi_s) = -\frac{U_0}{V_c},$$

where $\Delta f_r = f_r - f_{RF}$, and f_{RF} is the RF frequency.

If a high beam current is stored in a large storage ring, the frequency shift of the resonant frequency might be comparable, or even exceed the revolution frequency, f_0. This means that at some beam currents the coupling impedance of the accelerating mode at the upper synchrotron sidebands of the harmonics of the revolution frequency becomes significantly high and can cause coupled-bunch instability with very high growth rate (see, for example, [8], p. 4-4).

In case of CESR this frequency shift is shown for present 5-cell normal conducting copper RF (NRF) cavity and for single-cell superconducting RF cavity in Table 2. One can see that the frequency shift for NRF cavity is small enough for the total beam current up to 0.6 A which is the design value for that cavity. There is no visible limitation in case of SRF cavities. One should take into account this frequency shift while analyzing beam-cavity interaction. Due to the fact that RF system has amplitude feedback loop to keep V_c constant, there is no contribution to the incoherent frequency shift of the synchrotron frequency on RF harmonic of revolution frequency i.e. there is no compensation effect as it is for the HOMs. Apart from this frequency shift automatically provided by the control electronics of the RF system, there usually is an additional tuning offset which is equal to approximately $-10°$ or about -8.8 kHz according to recent measurements for CESR cavities [9].

4 Measurements in CESR, Comparison with Calculations, and Prediction for SRF Cavities

Measurements of the frequency shift for the lowest synchrotron sideband was performed recently in CESR [10]. We used positron beam consisting of 9 trains of 2 bunches per train with 28 nsec bunch spacing within a train. The synchrotron frequency at low current (2.6 mA in a single bunch) has been measured at 19.79 kHz. The total amplitude of RF voltage was kept at the level of approximately 6.2 MV. Figure 4 presents results of the measurements and calculations described below.

To calculate coherent frequency shift due to the fundamental RF mode one can use computer codes such as ZAP [11] and MBI [12]. The only inconvenience is that user has to correct the resonant frequency of the fundamental

Table 2: The shift of the cavity resonant frequency due to the beam loading for CESR cavities.

	5-cell NRF cavity: $V_c = 0.3$ MV/cell	BB1 single-cell SRF cavity: $V_c = 1.8$ MV/cell
I_{beam} [A]	Δf_r [kHz]	
0.1	-20.9	-1.22
0.2	-41.8	-2.44
0.3	-62.7	-3.65
0.4	-83.6	-4.87
0.5	-104.5	-6.09
0.6	-125.4	-7.31
0.7		-8.53
0.8		-9.75
0.9		-10.96
1.0		-12.2

mode according to (13) for every step in beam current. ZAP allows user to choose one of two formalisms, Zotter formalism or Wang formalism, to do multi-bunch instability calculations. Each formalism has its own criterion of applicability, but they both are satisfied for parameters of the CESR beam. One would expect to get the same results by using any of these formalisms. However, it has been found [13] that two formalisms have different coefficients for different modes of multi-bunch oscillations and for the dipole longitudinal case the ratio of two coefficients is equal to

$$\frac{Zotter\ \Delta\Omega}{Wang\ \Delta\Omega} = \frac{2\pi}{3} = 2.09...$$

It is somewhat confusing. In order to avoid long struggling with formulae I compared results of two programs, ZAP and MBI, for case of 7 symmetrically placed bunches. It turned out that results obtained with Wang formalism and MBI are in very good agreement. One should therefore use Zotter formalism with caution.

I should mention that, due to the dominant effect of fundamental RF mode and its high Q factor, the bunch pattern of the beam does not matter too much (as far as the bandwidth of the fundamental frequency resonance is less than bunch repetition frequency) so one can use almost arbitrary bunch pattern keeping the total beam current the same. ZAP can calculate growth rates and tune shifts only for a symmetric beam so I calculated $\Delta\Omega$s for a symmetric beam of 7 bunches. For MBI calculations I used 9 trains of 2 bunches with 28 nsec bunch spacing inside the train.

Also, I calculated frequency shift due to only the impedance of the fundamental mode near the RF harmonic of revolution frequency and took into account shift of the resonant frequency due to the beam loading (13):

$$\Delta\Omega \approx -\omega_s \frac{I_0}{2V_c \cos(\phi_s)} \left[ImZ_0^{\|}(h\omega_0 + \omega_s) + ImZ_0^{\|}(h\omega_0 - \omega_s) \right] \tag{14}$$

Figure 4 shows excellent agreement between MBI results and equation (14). An offset between ZAP results and MBI results is due to the different bunch pattern used in calculations. Slight disagreement between measurements and calculations indicates that actual parameters of the NRF cavities differ from what we assumed in Table 1. We restricted the beam current range to 300 mA because of the fact that the theory of coupled-bunch oscillations is valid until $\Delta\Omega \ll \omega_s$.

Now we can predict the synchrotron frequency shift for the SRF cavities. Results of calculations using formula (14) are shown in Figure 5. We see that coherent frequency shift due to the SRF cavities is much lower that shift due to the NRF cavities. One should note that the sign of the frequency shift for the SRF cavities is opposit to that for the NRF cavities. This is due to the fact that the sign depends on the relationship between the synchrotron frequency, ω_s, bandwidth of the resonance, and Δf_r. Figure 6 illustrates this relationship for the NRF and SRF cavities.

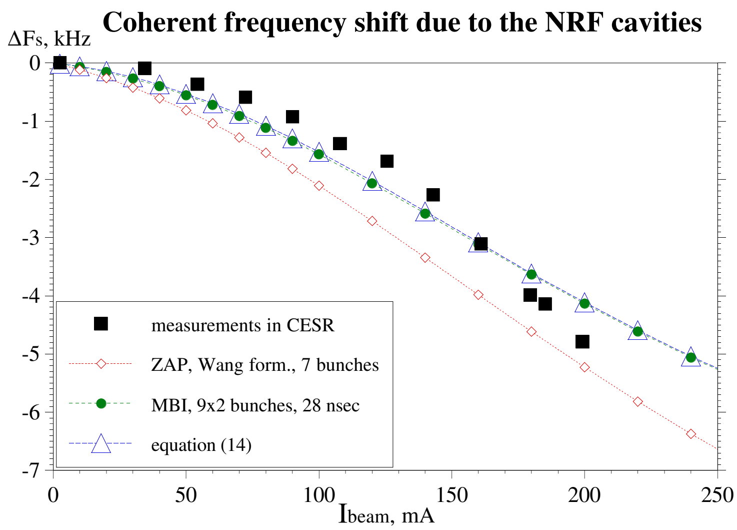

Figure 4: Measured and calculated frequency shift for the lowest synchrotron sideband.

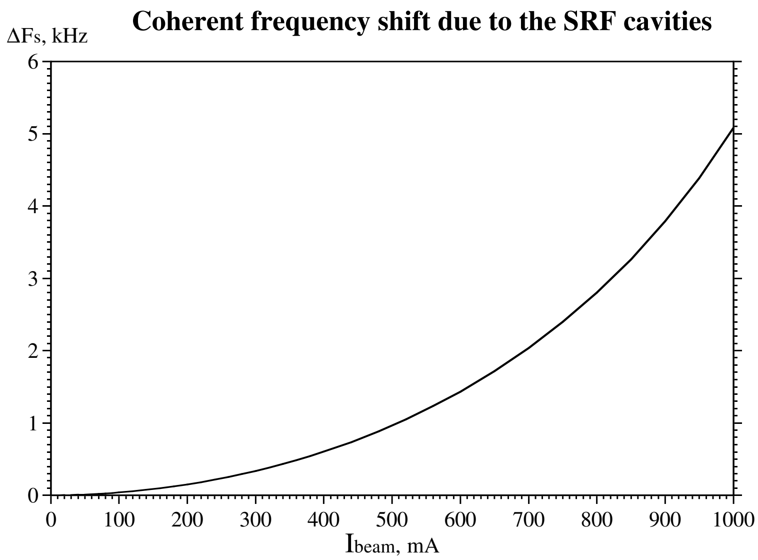

Figure 5: Prediction of the coherent frequency shift due to the SRF cavities.

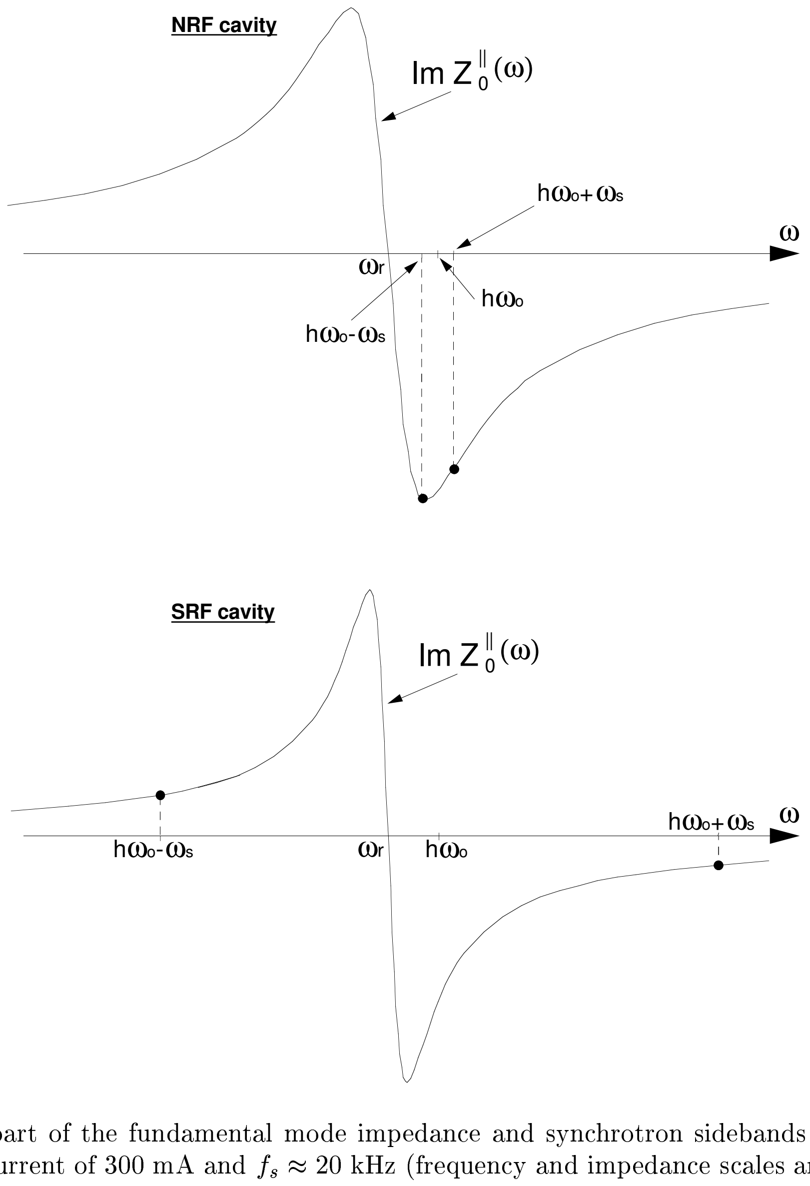

Figure 6: Imaginary part of the fundamental mode impedance and synchrotron sidebands for the NRF and SRF cavities at the beam current of 300 mA and $f_s \approx 20$ kHz (frequency and impedance scales are different).

5 Conclusion

The coherent synchrotron frequency shift due to the fundamental accelerating cavity mode has been measured at CESR as a function of beam current. Calculations have been performed using computer codes ZAP and MBI. Calculations are in a reasonably good agreement with measurements. Prediction of the coherent frequency shift has been obtained for the SRF cavities.

References

[1] CESR Impedance and Instabilities Machine Studies. http://cesrelog.lns.cornell.edu/mslog/impedance/

[2] B. Zotter. "Collective Effects - General Description," *Proceedings of the CERN Accelerator School on General Accelerator Physics,* Gif-sur-Yvette, Paris, France, 3-14 Sept. 1984, Report CERN 85-19, Vol. II, pp. 415-431 (27 November 1985).

[3] M. M. Karliner, et al. "Stability for the Phase Motion of a Relativistic Bunch in a Storage Ring," *J. of Technical Physics,* Vol. 38, No. 11, p. 1495 (1968) (in Russian). See English translation in *Sov. Phys. Tech. Phys.,* Vol. 13, No. 11, p. 1560 (1969).

[4] M. M. Karliner. "Multiple-bunch Phase Stability in Storage Ring," *J. of Technical Physics,* Vol. 41, No. 9, p. 1806 (1971) (in Russian). See English translation in *Sov. Phys. Tech. Phys.,* Vol. 16, No. 9, p. 1430 (1972).

[5] A. Chao. "Physics of Collective Beam Instabilities in High Energy Accelerators," *Wiley-Interscience Publication,* New York, 1993.

[6] M. M. Karliner, et al. "Longitudinal Stability of Colliding Beams in e^+e^- Storage Ring with the Account of Beam Coupling with the Environment," *Proceedings of the Third Advanced ICFA Workshop on Beam - Beam Effects in Circular Colliders,* p. 131, Novosibirsk, 1989.

[7] M. Billing, et al. "Measurement of Vacuum Chamber Impedance Effects on the Stored Beam at CESR," *Proceedings of the 1995 Particle Accelerator Conference and International Conference on High-Energy Accelerators,* Dallas, TX, May 1995, Vol. 4, pp. 3206-3208.

[8] "KEK B-Factory Design Report", KEK Report 95-7, August 1995.

[9] Calibration of Tuning Angles, May 27, 1996.
http://cesrelog.lns.cornell.edu/mslog/cesrrf/ms/tunangl_calibr_ibeam_960527.html

[10] Measurements of the Longitudinal Tune Shift as a Function of the Total Beam Current.
http://cesrelog.lns.cornell.edu/mslog/cesrrf/ms/fs_vs_ibeam_960527.html

[11] M. Zisman, et al. "ZAP User's Manual," Preprint LBL-21270, ESG-15, December 1986, also, Cornell LNS Report SRF/D 910118-7, January 1991.

[12] N. Mityanina. "MBI User's Manual," Cornell LNS Report SRF/D 970314-01 (1997).

[13] W. Hartung. Private communication, November 1995.